PROCEEDINGS of the
23rd International Congress on Acoustics

9 to 13 September 2019 in Aachen, Germany

A boundary virtual sound barrier system for sound radiation through openings with double-layer secondary sources and error microphones

Shuping WANG[1]; Xiaojun QIU[2]; Jiancheng TAO[3]

[1] University of Technology Sydney, Australia

[2] University of Technology Sydney, Australia

[3] Nanjing University, China

ABSTRACT

According to Huygens' principle, sound radiation through an opening can be completely reduced with a sufficient number of secondary sources over the entire opening, but secondary sources in the middle of the opening affect the functionalities of openings. In this paper, a boundary virtual sound barrier system is proposed. By applying double-layer secondary sources and error microphones both at the edge of the opening, such a system can achieve satisfactory noise reduction performance over a wide frequency band without blocking the opening. Experiments are carried out in the anechoic chamber to support the numerical simulation results.

Keywords: Virtual sound barrier, Boundary, Opening

1. INTRODUCTION

Openings are widely used in our lives to keep natural ventilation and lighting of buildings, but they provide sound transmission paths and result in the noise radiation problem at the same time. The active noise control (ANC) technique is a good supplement to traditional passive noise reduction methods in controlling sound radiation through openings because it performs better in low frequency range while passive noise control is more effective for high frequencies, and unlike passive noise control methods, it does not require the opening to be sealed (1).

Based on Huygens' principle, it has been proposed in previous work to implement secondary sources over the entire opening, and it is demonstrated as an effective way to reduce sound radiation through openings (2, 3); however, secondary sources in the middle of the opening still block the opening and affect its functionalities. It is desired that the ANC system be implemented at the edge of the opening to keep the opening completely clear. Wang *et al.* investigated the performance of a double-layer secondary source system at the edge of the opening, and found that it outperforms the single-layer system with the same number of secondary sources and there exists an upper-limit frequency for such a double-layer system, which is related to the size of the opening (4, 5). Bhan *et al.* also worked on the boundary layout of secondary sources and found that it could attenuate noise as effectively as the fully-glazed window (6).

In addition to the configuration of secondary sources, error sensing is another important part of ANC. To achieve global control, error microphones should provide signals proportional to the sound power. One way to obtain the sound power is to measure the sound intensity in the near field, but minimizing the near-field sound intensity suffers from the fact that it is a signed quantity (7). Qiu *et al.* compared eight different cost functions and found that the optimal cost function is the sum of the weighted mean active intensity in the direction normal to the surface surrounding the primary and secondary sources (8). In most cases, it is difficult to find the optimal locations for error microphones in the near field, and they are usually distributed over the entire opening to reduce noise radiation through the opening, which affect the functionalities of the opening as well (4).

[1] shuping.wang@uts.edu.au
[2] xiaojun.qiu@uts.edu.au
[3] jctao@nju.edu.cn

In our previous work, a double-layer boundary error sensing arrangement was proposed and numerical simulations showed that the double-layer arrangement performs better than single-layer one (9). More detailed numerical simulations are carried out in this paper to explore the rules of active control with double-layer error microphones at the edge. Experiments conducted in the anechoic chamber are presented to support the numerical simulation results.

2. MODEL

Figure 1 shows a schematic diagram of the proposed virtual sound barrier system at the edge of the cavity opening. In the system, secondary sources are distributed in two layers at the edge and they have the same coordinates in the *x*-*y* plane. Error microphones have similar layouts to the secondary sources and they are located above the secondary sources. The primary noise source is inside the open cavity. It is assumed that all the five walls are rigid, so sound outside is solely that transmitted through the opening.

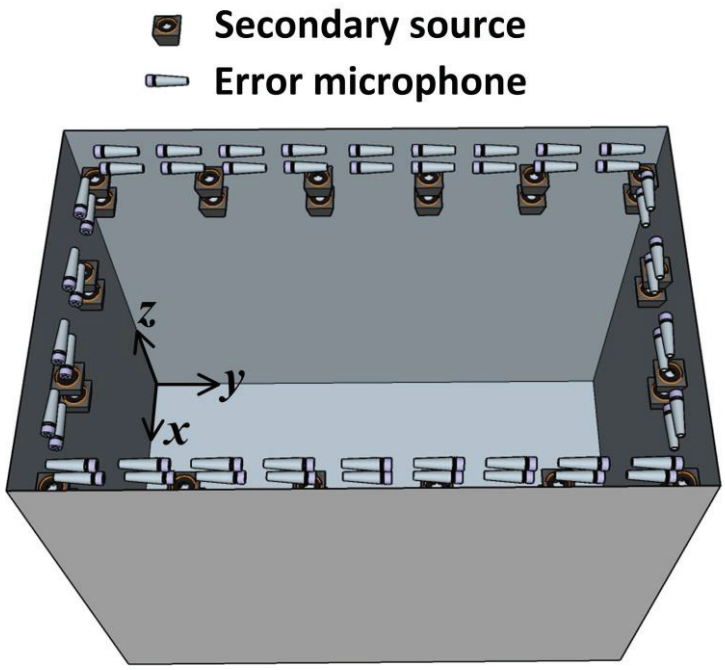

Figure – 1 The schematic diagram of the virtual sound barrier system at the edge of the cavity opening

As the opening is the only sound transmission path from inside the cavity to the outside, the sound power of the system can be calculated as an integral of sound intensity over the entire opening S. The sound power without active control is

$$W_{\text{off}} = \frac{1}{2}\iint_S \text{Re}\left\{p_{\text{po}}{}^{*} v_{\text{po}}\right\} \text{d}S\,, \tag{1}$$

where p_{po} and v_{po} are the primary sound pressures and particle velocities at the opening. The sound power with active control is the sum of the contributions of the primary source and all the secondary sources

$$W_{\text{on}} = \frac{1}{2}\iint_S \text{Re}\left\{[p_{\text{po}} + p_{\text{so}}]^{*}[v_{\text{po}} + v_{\text{so}}]\right\} \text{d}S\,, \tag{2}$$

where p_{so} and v_{so} are the secondary sound pressures and normal particle velocities at the opening. The noise reduction of the system is defined as the difference of the sound power level without and with control.

$$\text{NR} = 10\log_{10}\frac{W_{\text{off}}}{W_{\text{on}}}\,. \tag{3}$$

3. NUMERICAL SIMULATIONS

In the numerical simulations, the size of the open cavity is 0.432 m × 0.67 m × 0.598 m, and there are a total of 20 secondary sources at the edge of z = 0.448 m and z = 0.498 m planes. Three configurations of error microphones are investigated: single-layer, double-layer and evenly distributed, and their positions in the x-y plane are shown in Fig. 2. The single-layer and evenly distributed error microphones are at z = 0.588 m plane and the double-layer error microphones are at z = 0.568 m and z = 0.588 m planes. To prevent the system from being underdetermined, more error microphones than secondary sources are used, and the number is 32 here. The primary source is a monopole point source located at (0.1, 0.1, 0.1) m inside the open cavity with a strength of 10^{-4} m^3/s.

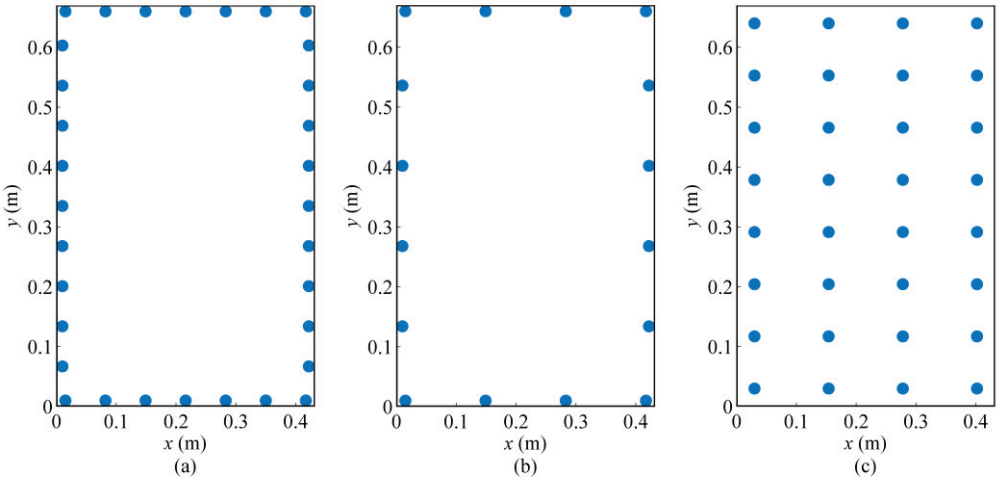

Figure – 2 The positions of error microphones in the x-y plane: (a) the single-layer configuration, (b) the double-layer configuration, (c) the evenly distributed configuration

The sum of the squared sound pressures at the error points is used as the cost function to obtain the strengths of secondary sources (10). The noise reduction of the system is calculated with Eq. (3). Figure 3 shows the sound power levels with and without control under the three configurations of error microphones. It is clear that the system with error microphones evenly distributed over the entire opening achieves the best noise reduction performance, and the one with double-layer error microphones outperforms that with single-layer ones at all the frequencies below 1000 Hz.

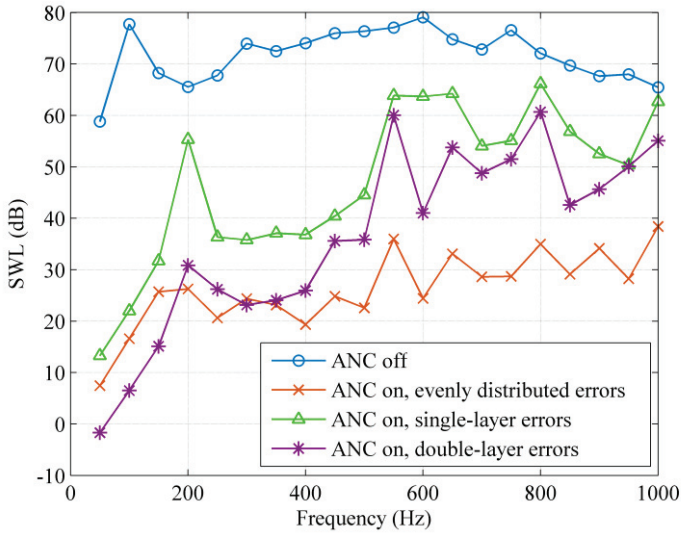

Figure – 3 The sound power levels with and without control when 20 secondary sources are arranged in double-layer configuration

The effect of the heights of double-layer error microphones on the noise reduction performance is also investigated. There are still a total of 32 error microphones. Figure 4(a) shows the sound power levels with and without control when the distance between the two layers is fixed as 0.02 m, and it can be seen that the noise reduction performance improves when the error microphones are closer to the opening. If one of the layers is fixed at z = 0.518 m, and the other layer is placed at different heights, the sound power levels with and without control are shown in Fig. 4(b). Although all the configurations achieve satisfactory noise reductions below 1000 Hz in Fig. 4(b), there are still small differences between them and the system with the other layer closer to the opening performs the best.

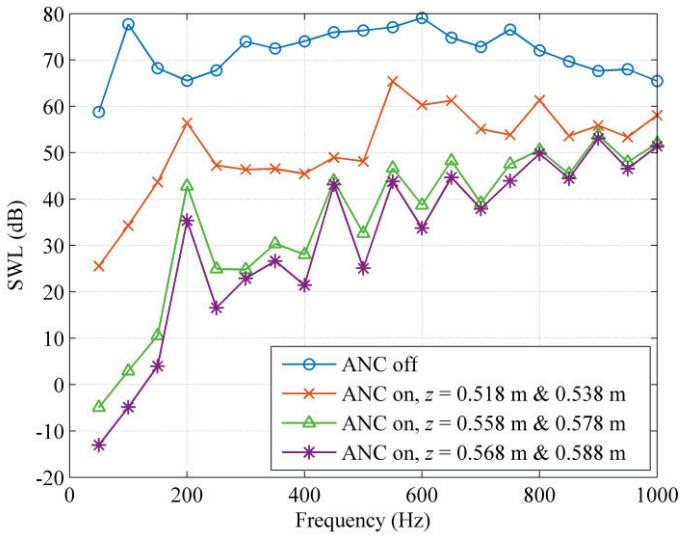

(a)

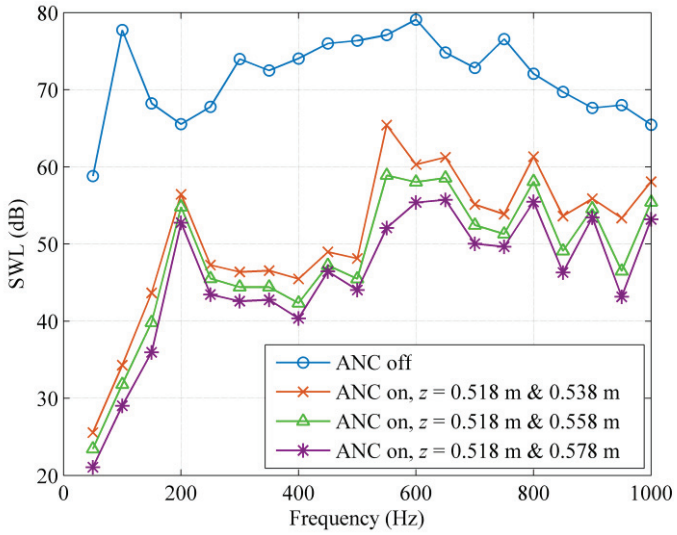

(b)

Figure – 4 The sound power levels with and without control with 20 double-layer secondary sources and 32 double-layer error microphones: (a) the distance between two layers of error microphones is fixed as 0.02 m, (b) one of the layers is fixed at z = 0.518 m plane

Double layer error microphones also perform better than single-layer ones when the primary sound field is complicated. The primary source is simulated as 8 monopole point sources in a 0.1 m × 0.1 m × 0.1 m volume with random amplitudes and phases. Figure 5 shows the results for 32 single-layer and double-layer error microphones. It is clear that the system with double-layer error microphones achieves higher noise reductions than that with single-layer ones.

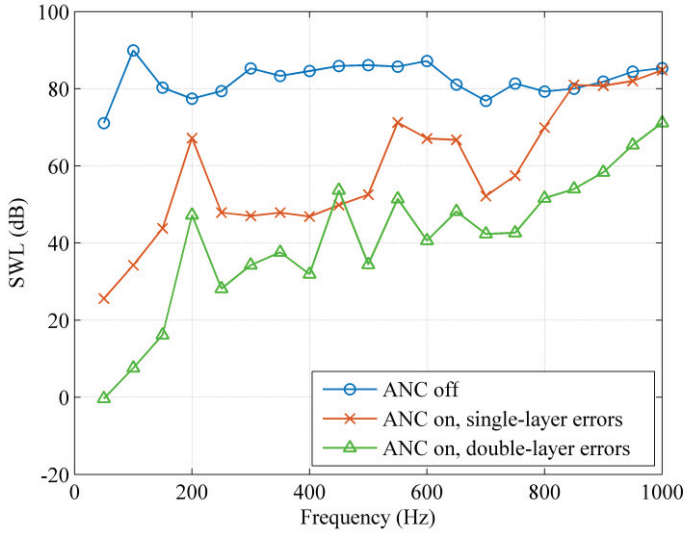

Figure – 5 The sound power levels with and without control with 20 double-layer secondary sources and 32 double-layer error microphones when the primary sound field is complicated

4. EXPERIMENTS

Experiments were carried out in the anechoic chamber of Nanjing University. The open cavity was constructed with five 20 mm-thick acrylic glass plates and the size is 0.432 m × 0.67 m × 0.598 m. A total of 32 secondary sources were implemented at the edge of $z = 0.448$ m and $z = 0.548$ m planes. The primary source was a loudspeaker inside the open cavity which generated tonal sound field. Three configurations of error microphones: evenly distributed, single-layer and double-layer were investigated and the pictures of the three experimental setups are shown in Figs. 6(a)-(c). The single-layer and evenly distributed error microphones were installed in the opening plane. The double-layer error microphones were installed at the opening and the plane 0.02 m below it. The waveform synthesis algorithm was used in the experiments; it applied the internally synthesized tonal signal as the reference signal, so no reference microphone was required here (11). As shown in Fig. 6(d), ten microphones fixed on a frame with a radius of 1.5 m were used to measure the sound power levels with and without control (12).

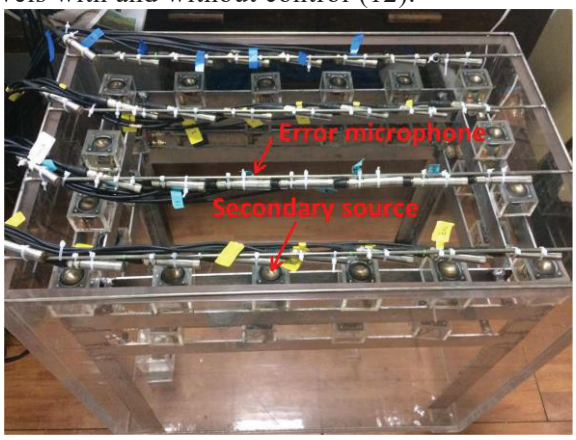

(a)

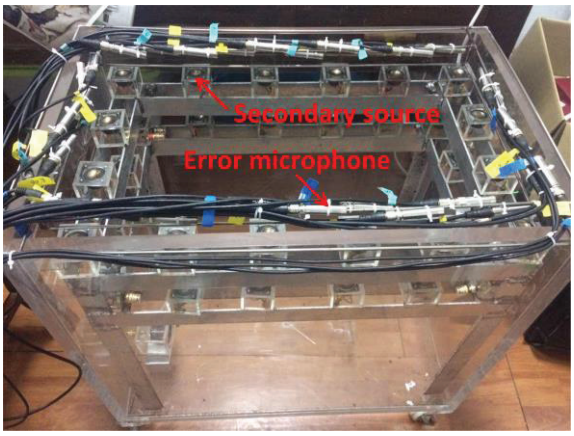

(b)

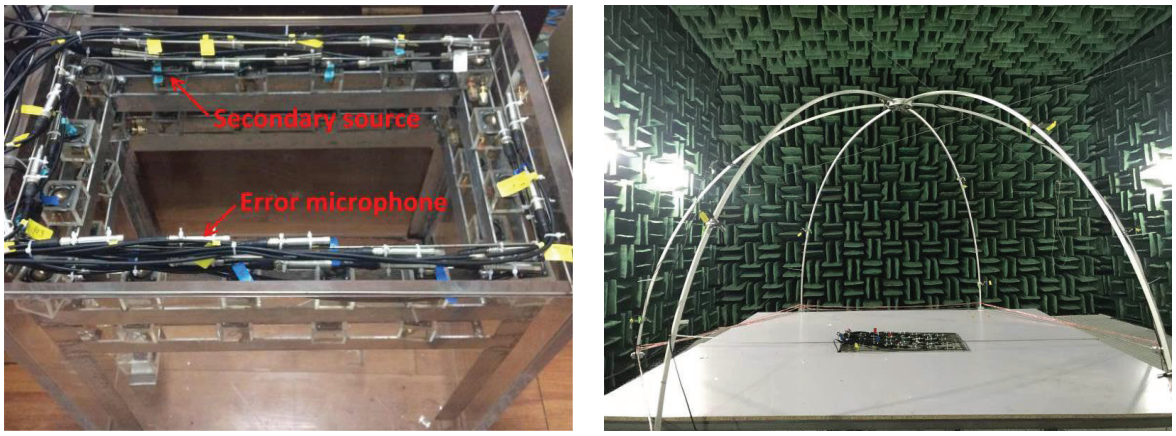

(c) (d)

Figure – 6 Pictures of the experimental setup: (a) evenly distributed error microphones, (b) single-layer error microphones, (c) double-layer error microphones, (d) the panoramic view in the anechoic chamber

The sound power levels measured in the experiments with and without control are shown in Fig. 7(a) and the corresponding numerical simulation results on the same configurations are shown in Fig. 7(b). It can be seen from Fig. 7(a) that the system with evenly distributed error microphones achieve the best performance among the three configurations and the double-layer error microphones perform slightly better than the single-layer ones.

It can be found by comparing Fig. 7(a) with Fig. 7(b) that the advantage of the double-layer error microphones over single-layer ones in the experiments is not as apparent as that in the numerical simulations. There are two possible reasons. One is that the error microphones used in the experiments have different sensitivities, and it is actually the sum of the squared electric signals picked up by the error microphones instead of the sum of the squared sound pressures at error points that is minimized in the experiments, which makes the noise reduction performance different from that in the numerical simulations. The other possible reason is that the error microphones in the experiments were not rigorously fixed at the positions they were supposed to be at. The reasons will be checked in the future. Future work also includes finding a proper way to pick up the reference signal, especially for practical sound fields.

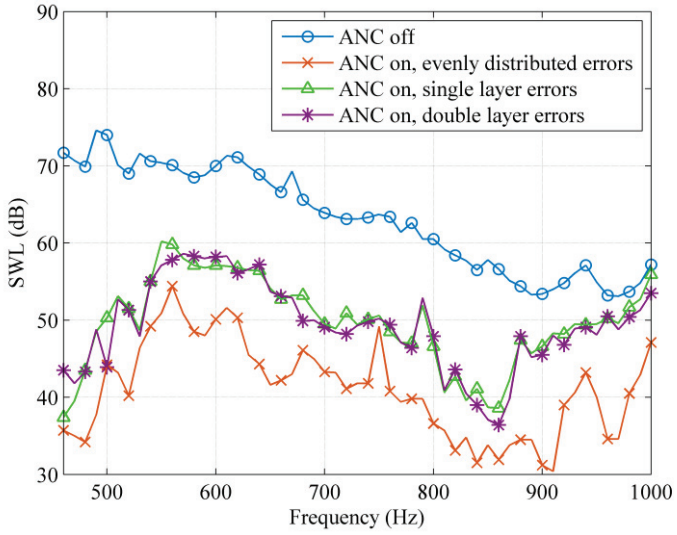

(a)

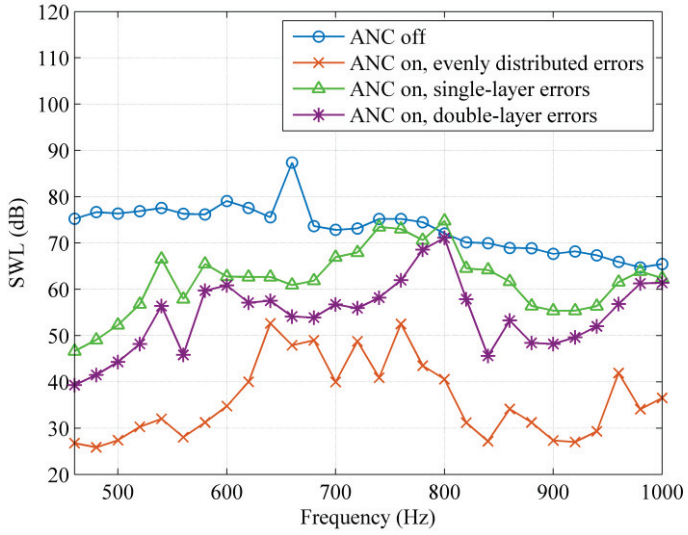

(b)

Figure – 7 The sound power levels with and without control: (a) experimental results, (b) corresponding numerical simulation results

5. CONCLUSIONS

A boundary virtual sound barrier system with both double-layer secondary sources and error microphones at the edge is proposed to reduce sound radiation through openings. Numerical simulations show that similar to the conclusions for secondary source configurations, the system with double-layer error microphones performs better than that with single-layer ones, and the conclusion is still valid for complicated primary sound fields. It is also found that the performance of the system with double-layer error microphones improves if the error microphones are closer to the opening. Experimental results in the anechoic chamber show that the system with double-layer error microphones perform slightly better than that with single-layer ones, and the advantage is not as apparent as that in the numerical simulations. The reasons might be the different sensitivities and inaccurate positions of error microphones in the experiments.

ACKNOWLEDGEMENTS

This research was supported by the National Science Foundation of China (11874218, 11474163) and under the Australian Research Council's Linkage Projects funding scheme (LP140100987). The authors would also like to thank Mr. Kang Wang for his help with the experiments.

REFERENCES

1. De Salis M, Oldham D, Sharples S. Noise strategies for naturally ventilated buildings. Build Environ. 2002;37(5):471-84.
2. Murao T, Nishimura M, He J, Lam B, Ranjan R, Shi C, Gan W. Feasibility study on decentralized control system for active acoustic shielding. Proc Inter-noise; 21-24 August 2016; Hamburg, Germany 2016. p. 462-71.
3. Lam B, Shi C, Gan W. Active noise control systems for open windows: current updates and future perspectives. Proc ICSV; 23-27 July 2017; London, UK 2017. p. 1-7.
4. Wang S, Tao J, Qiu X. Controlling sound radiation through an opening with secondary loudspeakers along its boundaries. Sci Rep. 2017;7:2836-47.
5. Wang S, Tao J, Qiu X, Pan J. Mechanisms of active control of sound radiation from an opening with boundary installed secondary sources. J Acoust Soc Am. 2018;143(6):3345-51.
6. Lam B, Shi C, Shi D, Gan W. Active control of sound through full-sized open windows. Build Environ. 2018;141:16-27.
7. Berry A, Qiu X, Hansen C. Near-field sensing strategies for the active control of the sound radiated from a plate. J Acoust Soc Am. 1999;106(6):3394-406.

8. Qiu X, Hansen C, Li X. A comparison of near-field acoustic error sensing strategies for the active control of harmonic free field sound radiation. J Sound Vib. 1998;215(1):81-103.
9. Wang S, Tao J, Qiu X, Pan J. Controlling sound radiation through openings with an active noise control system at the edge. Proc Inter-noise; 26-29 August 2018; Chicago, USA 2018.
10. Nelson P, Elliott S. Active Control of Sound. 2nd ed. New York, USA: Academic; 1992.
11. Qiu X, Hansen C. An algorithm for active control of transformer noise with on-line cancellatio npath modelling based on the perturbation method. J Sound Vib. 2001;240(4):647-65.
12. ISO 3744: Acoustics-Determination of sound power levels of noise sources using sound pressure-Engineering method in an essentially free field over a reflecting plane. International organization for standardization, Geneva, Switzerland. 1994.